

# Gate-controlled current switch in graphene

Kimmo Sääskilahti and Ari Harju\*

*Helsinki Institute of Physics and Department of Applied Physics,  
Helsinki University of Technology, P.O.Box 4100, FI-02015 TKK, Finland*

Pirjo Pasanen<sup>†</sup>

*Nokia Research Center, P.O.Box 407, FI-00045 Nokia Group, Finland*

(Dated: May 30, 2019)

We study numerically cross conductances in a four-terminal all-graphene setup. We show that far away from the Dirac point current flows along zigzag directions, giving the possibility to guide the current between terminals using a tunable pn-junction. The device operates as a gate-controlled current switch, and the electronic properties of graphene are crucial for efficient performance.

PACS numbers: 73.23.-b, 73.63.-b

Graphene, the two-dimensional form of carbon, has been creating a lot of interest not only in the physics community but also in the electronic industry, due to its extraordinary physical properties [1, 2, 3]. These properties include, for example, exceptionally high charge mobility, room temperature ballistic transport, ultrahigh thermal conductivity and mechanical strength. High charge mobilities and ballistic transport are found also in other semiconductor materials such as GaAs, but due to the relatively high costs and the toxicity of the materials they have not been adopted for extensive use in mass manufactured consumer electronic devices. Provided that the manufacturing questions will be resolved, in the long term graphene could be used as material for high-performance nanoelectronic devices, even on flexible and transparent substrates.

In addition to graphene nanoribbon field effect transistors [4] and transistors for analog applications [5], the semi-metallic band structure and the peculiar linear dispersion relation of the graphene charge carriers [6] can enable novel types of electronic devices to be constructed. The first experimental demonstrations of graphene specific devices have already been reported: a frequency multiplication based on switching between electron and hole conduction [7] and a digital logic inverter [8].

Keeping in mind the ultimate goal of building all-graphene circuits it is important to study also the electric properties of more complex geometrical structures. Multiterminal graphene devices have been studied theoretically in [9, 10]. It was shown that near the Dirac point evanescent modes lead to quantum corrections in the multiterminal cross correlations [10], and that cross conductances in graphene T-junctions are highly sensitive to the symmetry of interconnections [9]. Effects like these are interesting, since they probe the unique electronic properties of graphene. One of the most unusual and interesting consequences of the quasi-relativistic electron dynamics is the Klein tunneling [11, 12, 13]. The effect entails that electrons incoming to a potential barrier in graphene can couple to the hole states inside the

barrier and transmit through perfectly. This is related to the fact that backscattering is strictly forbidden in clean graphene pn-junctions [14]. Experimental evidences of Klein tunneling have been reported by [15, 16]. Theoretically, graphene nanodevices based on manipulating charge carriers by potential barriers have been proposed in [17, 18].

In this letter, we study multiterminal conductances in a four-terminal geometry and see how the intricate properties of graphene can be exploited even further. We show, for example, that the cross conductances between different terminals can be tuned by a step potential. In other words, the device performs as a current switch controlled by a top gate. The band structure induced by the honeycomb lattice and the closely related relativistic dynamics are critical to the performance of the device.

The studied geometry is shown in Fig. 1. The central region (device area) is a rectangular graphene island. The size of the the island is given by a pair of numbers  $(N_a, N_z)$ , where  $N_a$  ( $N_z$ ) is the number of outermost atoms on the armchair (zigzag) edge, as shown in the figure. The width of the device is  $W/a = \sqrt{3}N_z$

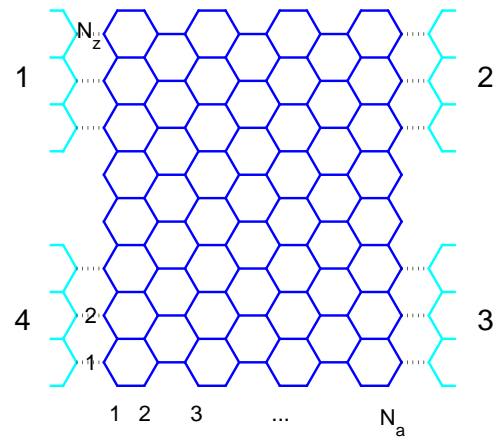


FIG. 1: (Color online) The setup for an  $(N_a, N_z)$  device.

and the length  $L/a = 3N_a/2$ , where  $a \approx 0.142$  nm is the carbon-carbon distance. We attach left-right symmetric armchair leads onto the four corners of the island and study the resulting cross conductances between the four terminals. One can view the first terminal acting as a source of electrons, and our aim is to control the current to one of the other leads.

We calculate the currents in the linear response and zero temperature regime, as described by Datta [19]. The retarded Green's function for the device area is given by

$$G^R(E) = \left[ (E + i0^+) - H_D - \sum_{\alpha=1}^4 \Sigma_{\alpha}^R(E) \right]^{-1}, \quad (1)$$

where  $H_D$  is the tight-binding Hamiltonian for the device area and  $\{\Sigma_{\alpha}^R\}_{\alpha=1}^4$  are the self-energies describing the four semi-infinite leads. The tight-binding Hamiltonian is

$$H_D = - \sum_{i,j} t_{ij} c_i^{\dagger} c_j, \quad (2)$$

where  $t_{ij} = t \approx 2.7$  eV for nearest neighbors and zero otherwise. The self-energies are calculated using a standard decimation routine [20]. The relevant energy range is given by a "back gate" that fixes the overall Fermi level of the system under study. In the following, we suppress the energy dependence of all quantities.

The cross conductance between leads  $\alpha$  and  $\beta$  is given by [21]

$$G_{\alpha\beta} = - \frac{dI_{\alpha}}{dV_{\beta}} = \frac{2e^2}{h} \text{Tr} \left[ \mathbf{s}_{\alpha\beta}^{\dagger} \mathbf{s}_{\alpha\beta} \right], \quad (3)$$

where  $\mathbf{s}_{\alpha\beta}$  are the scattering matrices. In the absence of magnetic field, the cross conductances satisfy the reciprocity relation  $G_{\alpha\beta} = G_{\beta\alpha}$ , so the ordering of indices is irrelevant. The traces are calculated using the formula

$$G_{\alpha\beta} = \frac{2e^2}{h} \text{Tr} \left[ \Gamma_{\alpha} G^R \Gamma_{\beta} (G^R)^{\dagger} \right], \quad (4)$$

where the coupling matrices are given by the imaginary parts of the self-energies, i.e.  $\Gamma_{\alpha} = i \left( \Sigma_{\alpha}^R - (\Sigma_{\alpha}^R)^{\dagger} \right)$ . Since we are working in linear response, we refer to "current" and "conductance" interchangeably.

Let us start the analysis by looking at the effects of geometry. The width of device is fixed to be  $N_z = 52$  and we choose leads such that each lead is connected to 13 atoms in the zigzag edges. For small Fermi energies, the current is nearly evenly distributed between all terminals (see below). However, for a high Fermi level one starts to see direction-dependent effects.

The results for cross conductances at  $E_F = 0.8t$  as a function of the junction length  $N_a$  are shown in Fig. 2. The conductances are given in units of the conductance quantum  $G_Q = 2e^2/h$ . There are nine propagating

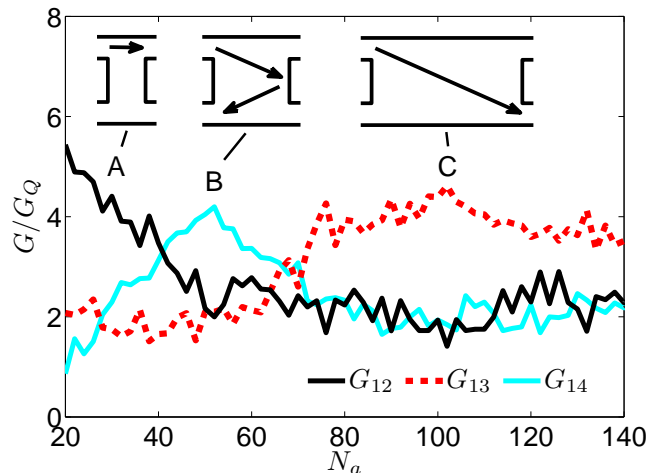


FIG. 2: (Color online) The cross conductances as a function of the length  $N_a$  for a device area with width  $N_z = 52$ . Fermi level is at  $E_F = 0.8t$ . Insets: Schematic representations of the current flow for selected aspect ratios (A-C).

modes in the leads which is the maximum total transmission for leads of this width. Figure 2 shows many interesting features. In a short junction, the dominating cross conductance is  $G_{12}$ . This means that most of the current travels straight from the terminal 1 to the terminal 2, as could be expected (point A in the figure). Increasing the length makes the cross conductance  $G_{12}$  smaller until at  $N_a \sim 50$  the cross conductance  $G_{14}$  peaks (point B). This can be interpreted as a reflection from the opposite wall, giving the first hint that the flow of current is not chaotic by nature.

When the length of the junction is still increased, the cross conductance  $G_{13}$  starts to increase, peaking at  $N_a \approx 100$  (point C). Interestingly, this corresponds to an aspect ratio of  $\tan^{-1}(W/L) = 30^\circ$ . This proves that for this high a Fermi level, the current has a strong tendency to propagate along the zigzag path from terminal 1 to terminal 3. This is due to trigonal warping in the two non-equivalent corner points of the Brillouin zone [2].

In the rest of the paper, we study how we can control the direction of the current using a potential step. In our notation, the requirement  $L = \sqrt{3}W$  means roughly  $N_a = 2N_z$ , so for the rest of the paper we fix the geometry to be (104, 52). It is good to remember that armchair edges cause intervalley scattering and are therefore rather important in focusing the current effectively along specific lattice directions, by making one of the corner points in the Brillouin zone to be preferred over the other.

The cross conductances as a function of the Fermi level for a (104, 52)-junction are shown in Fig. 3. For  $E_F \lesssim 0.5t$  cross conductances are nearly equal, indicating that all terminals are equally probable points for exit. Thus the behaviour of the currents inside the rectangular middle area could be described as chaotic. This is

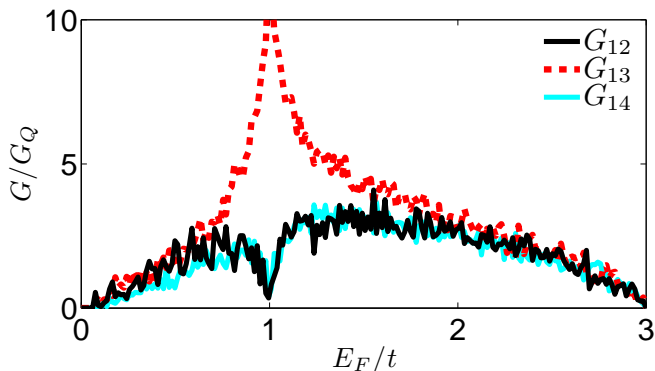


FIG. 3: (Color online) The cross conductances as a function of the Fermi level for a (104, 52)-junction. The zigzag direction is preferred only near  $E_F = t$ .

not surprising, since the relativistic dynamics in rectangular dots is known to be non-integrable [22]. Only when  $E_F \gtrsim 0.5t$  starts the cross conductance  $G_{13}$  to dominate due to the tendency to propagate along the zigzag path. This requires the Fermi level to be rather high, since in the Dirac cone all directions are on equal footing, and to get out of this regime the Fermi wavelength must be reduced to be of the same order as the lattice constant.

Now we introduce a potential step in the middle of the island. The results for the cross conductances as a function of the height of the step are shown in Fig. 4. The shape of the potential is  $V(x) = V[1 + \exp(-2x/d)]^{-1}$  with a smoothing factor  $d = a$ . This is a very steep barrier, and one gets practically the same results for  $d \rightarrow 0$ . In Fig. 4, one can see three regions of primary interest: (i) For  $V \lesssim 0$  the current flows mainly to terminal 3 due to the tendency to propagate along the zigzag path. (ii) For  $V \approx 0.8t$  the right part of the system is at the Dirac point and most of the current is reflected from the barrier to terminal 4. The evanescent modes do not contribute here, since also the semi-infinite leads in terminals 2 and 3 are at the Dirac point. (iii) For  $V \approx 2E_F$  the barrier works as a Veselago lens with a refractive index  $n = -1$ , and the current transmits to terminal 2.

To understand the difference between points (i) and (iii), let us briefly review the principle of Veselago lensing [23]. Consider a case in which the left half of the graphene island is at chemical potential  $\mu_L$  and the right half at  $\mu_R = -\mu_L$ , meaning that there is a symmetric np-junction in the middle of the island. Incoming electrons with a propagation angle  $\theta$  can tunnel through the barrier as holes. The propagation angle of the outgoing hole is then  $\theta' = -\theta$ , since the conservation of transverse momentum requires  $k_c \sin \theta = -k_v \sin \theta'$ , where  $k_c$  and  $k_v$  are the Fermi wave vectors in the  $n$  and  $p$  regions, respectively. Thus the barrier works as a Veselago lens with a refractive index  $n = -1$ , meaning that we can focus the charge carriers to terminal 2 instead of terminal

3. Note that the maximum of  $G_{12}$  is roughly 3/4 of the maximum of  $G_{13}$ , indicating an approximate probability of 3/4 for transmission through the np-junction. This is in reasonable agreement with the theoretical value of  $T = \cos^2 30^\circ = 3/4$ .

In Fig. 5, we show the cross conductances when the smoothing of the step is increased up to  $d = 10a$ . Theoretically, this would mean that the transmission probability  $T = \cos^2 \theta$  is replaced by  $T = \exp(-\pi k_F \tilde{d} \sin^2 \theta)$ , where  $\tilde{d}$  is the effective length scale of the step and  $k_F$  is the Fermi wave vector [24]. The assumption of smoothness requires  $k_F \tilde{d} \gg 1$ . As a consequence, when  $V = 2E_F \approx 1.6t$ , the cross conductance  $G_{12}$  is notably smaller than for a steep junction (Fig. 4). The reflected current  $G_{14}$  is naturally larger in this case. It is important to remember, of course, that theoretical calculations are done in the limit of long wavelengths and low energies where the continuum approach using the Dirac equation is valid. Hence these results are not rigorously applicable in our case, but entail the relevant physics.

Note that even in the case of a smooth barrier one may be able to switch the current between terminals. By using  $V \approx E_F$  one can guide the current effectively to terminal 4 since in this case the right part of the device is at the Dirac point. Knowing that the "total" conductance is  $9G_Q$ , we see that approximately 2/3 of the incoming current is reflected to terminal 4 and 1/3 traverses back to terminal 1. One can also steer the currents between terminals 2 ( $V \approx 2E_F$ ) and 3 ( $V \approx 0$ ) even if the cross-conductance  $G_{14}$  dominates. For effec-

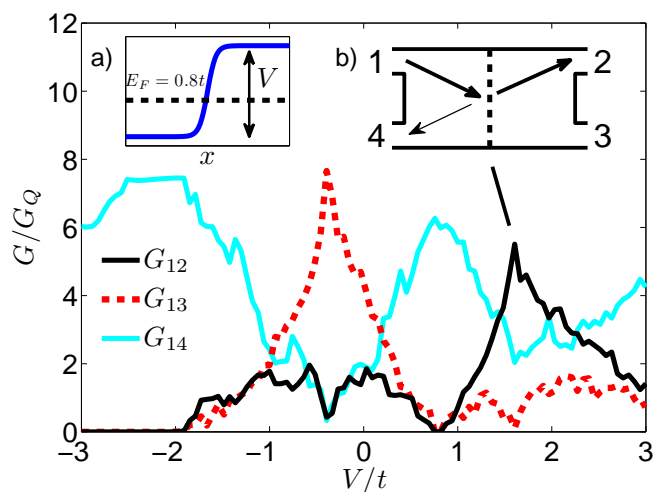


FIG. 4: (Color online) The cross conductances as a function of the step height  $V$  for a steep potential barrier. The central region is of size (104, 52). Insets: a) Energy diagram in the longitudinal direction. b) Schematic representation of the current flow for  $V = 2E_F$ . The barrier works as a Veselago lens with refractive index  $n = -1$ , focusing the current to terminal 2. Part of the current is reflected to terminal 4.

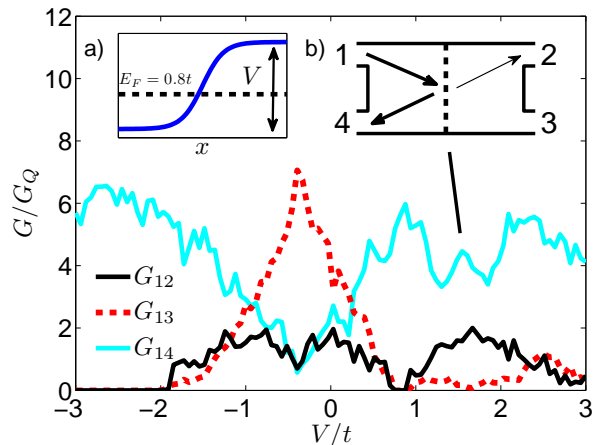


FIG. 5: (Color online) The cross conductances as a function of the step height  $V$  for a smooth potential barrier. The smoothing factor is  $d = 10a$ . Insets: a) Energy diagram in the longitudinal direction. b) Schematic representation of the current flow for  $V = 2E_F$ . In case of a smooth barrier, most of the current is reflected.

tive switching between terminals we only require, after all, that  $G_{12} \gg G_{13}$  for  $V = 2E_F$ .

It is worth mentioning that we have considered a symmetric structure, in which the number of atoms in the leads in the transverse direction is odd. Due to the small size of the computational domain, the effects of breaking this symmetry are significant. The precise form of the leads is not, however, critical to our results: one can reproduce qualitatively similar results in the entire energy range using square lattice leads, when the local potential in the leads is chosen to correspond to a good description of contacts [25].

We have also studied the effect of interface disorder on the performance. When the hopping parameters from the leads to the central region are replaced by  $t \rightarrow t + \gamma$ , where  $\gamma$  is a uniformly distributed random number from the interval  $[-0.5t, 0.5t]$ , the results remain qualitatively the same. Only the magnitudes of the cross conductances are slightly decreased. The effect of bulk disorder may be more important. Short-range disorder potential causes intervalley scattering which effectively hinders the performance of the device by reducing the preferrability of a specific zigzag direction. Also intravalley scattering is harmful, since it causes the quasiparticles to scatter inside the tridiagonally warped valley away from the  $\Gamma - K$  direction.

In conclusion, we have studied cross conductances in a four-probe all-graphene system. It was shown that in our setup aspect ratios of  $\tan^{-1}(W/L) = 30^\circ$  lead to strong turning currents due to the preference of current to propagate along a zigzag path, when the Fermi level is

high. Once this situation is realized, the current can be controlled by introducing a potential step in the middle of the island. Smoothing the potential destroys Veselago lensing to some degree, but even in this case one can achieve switching between two terminals. The fact that the leads were connected to zigzag edges is important, and we leave studies on different kinds of setups for future work.

We thank all members of the NOKIA/TKK graphene collaboration for helpful discussions.

\* URL: <http://tfy.tkk.fi/qmp>

† URL: <http://research.nokia.com/>

- [1] A. Geim and K. S. Novoselov, *Nature Mater.* **6**, 183 (2007).
- [2] A. H. Castro Neto, F. Guinea, N. M. R. Peres, K. S. Novoselov, and A. K. Geim, *Rev. Mod. Phys.* **81**, 109 (2009).
- [3] K. S. Novoselov *et al.*, *Science* **306**, 666 (2004).
- [4] M. Lemme, T. Echtermeyer, M. Baus, and H. Kurz, *El. Dev. Lett., IEEE* **28**, 282 (2007).
- [5] Y.-M. Lin *et al.*, *Nano Lett.* **9**, 422 (2009).
- [6] P. R. Wallace, *Phys. Rev.* **71**, 622 (1947).
- [7] H. Wang, D. Nezich, J. Kong, and T. Palacios, *El. Dev. Lett., IEEE* **30**, 547 (2009).
- [8] F. Traversi, V. Russo, and R. Sordan, *Appl. Phys. Lett.* **94**, 223312 (2009).
- [9] Y. P. Chen, Y. E. Xie, L. Z. Sun, and J. Zhong, *Appl. Phys. Lett.* **93**, 092104 (2008).
- [10] M. A. Laakso and T. T. Heikkilä, *Phys. Rev. B* **78**, 205420 (2008).
- [11] C. W. J. Beenakker, *Rev. Mod. Phys.* **80**, 1337 (2008).
- [12] M. I. Katsnelson, K. S. Novoselov, and A. K. Geim, *Nature Phys.* **2**, 620 (2006).
- [13] O. Klein, *Z. Phys.* **53**, 157 (1929).
- [14] T. Ando, T. Nakanishi, and R. Saito, *J. Phys. Soc. Jpn.* **67**, 2857 (1998).
- [15] N. Stander, B. Huard, and D. Goldhaber-Gordon, *Phys. Rev. Lett.* **102**, 026807 (2009).
- [16] A. F. Young and P. Kim, *Nature Phys.* **5**, 222 (2009).
- [17] V. V. Cheianov, V. Fal'ko, and B. L. Altshuler, *Science* **315**, 1252 (2007).
- [18] A. Cresti, *Nanotechnology* **19**, 265401 (2008).
- [19] S. Datta, *Electronic Transport in Mesoscopic Systems* (Cambridge University Press, Cambridge, England, 2002).
- [20] M. P. López Sancho, J. M. López Sancho, and J. Rubio, *J. Phys. F: Met. Phys.* **15**, 851 (1985).
- [21] M. Büttiker, *Phys. Rev. B* **46**, 12485 (1992).
- [22] M. V. Berry and R. J. Mondragon, *Proc. R. Soc. A* **412**, 53 (1987).
- [23] V. G. Veselago, *Sov. Phys. Usp.* **10**, 509 (1968).
- [24] V. V. Cheianov and V. I. Fal'ko, *Phys. Rev. B* **74**, 041403(R) (2006).
- [25] H. Schomerus, *Phys. Rev. B* **76**, 045433 (2007).